9-2-2005

Arginine methylation of yeast mRNA-binding protein Npl3 directly affects its function, nuclear export, and intranuclear protein interactions

Anne E. McBride
Bowdoin College

Jeffrey T. Cook
Bowdoin College

Elizabeth A. Stemmler
Bowdoin College

Kate L. Rutledge
Bowdoin College

Kelly A. McGrath
Bowdoin College

See next page for additional authors

THE JOURNAL OF BIOLOGICAL CHEMISTRY
Vol. 280, No. 35, Issue of September 2, pp. 30888–30898, 2005
Printed in U.S.A.

Arginine Methylation of Yeast mRNA-binding Protein Npl3 Directly Affects Its Function, Nuclear Export, and Intranuclear Protein Interactions*[S]

Received for publication, May 27, 2005, and in revised form, June 30, 2005
Published, JBC Papers in Press, July 5, 2005, DOI 10.1074/jbc.M505831200

Anne E. McBride‡, Jeffrey T. Cook§, Elizabeth A. Stemmler, Kate L. Rutledge, Kelly A. McGrath, and Jeffrey A. Rubens

From the Departments of Biology and Chemistry, Bowdoin College, Brunswick, Maine 04011

Arginine methylation can affect both nucleocytoplasmic transport and protein-protein interactions of RNA-binding proteins. These effects are seen in cells that lack the yeast hnRNP methyltransferase (HMT1), raising the question of whether effects on specific proteins are direct or indirect. The presence of multiple arginines in individual methylated proteins also raises the question of whether overall methylation or methylation of a subset of arginines affects protein function. We have used the yeast mRNA-binding protein Npl3 to address these questions *in vivo*. Matrix-assisted laser desorption/ionization Fourier transform mass spectrometry was used to identify 17 methylated arginines in Npl3 purified from yeast: whereas 10 Arg-Gly-Gly (RGG) tripeptides were exclusively dimethylated, variable levels of methylation were found for 5 RGG and 2 RG motif arginines. We constructed a set of Npl3 proteins in which subsets of the RGG arginines were mutated to lysine. Expression of these mutant proteins as the sole form of Npl3 specifically affected growth of a strain that requires Hmt1. Although decreased growth generally correlated with increased numbers of Arg-to-Lys mutations, lysine substitutions in the N terminus of the RGG domain showed more severe effects. Npl3 with all 15 RGG arginines mutated to lysine exited the nucleus independent of Hmt1, indicating a direct effect of methylation on Npl3 transport. These mutations also resulted in a decreased, methylation-independent interaction of Npl3 with transcription elongation factor Tho2 and inhibited Npl3 self-association. These results support a model in which arginine methylation facilitates Npl3 export directly by weakening contacts with nuclear proteins.

Protein-arginine methylation by type I methyltransferases, which add one or two methyl groups to one of the guanidino nitrogens of arginine, has been shown to affect a number of eukaryotic processes including protein transport, transcription, and cell signaling (reviewed in Refs. 1–3). Although many substrates for arginine methyltransferases are RNA-binding proteins, to date methylation has been shown to have only relatively minor effects on the affinity of target proteins for RNA (4–7). Many studies, however, point to a role for arginine methylation in modulating protein-protein interactions (reviewed in Ref. 2). The observation of both positive and negative effects of arginine methylation on protein-protein interactions has led to models for roles of arginine methylation in cell signaling and transcription, through the modification of histones, RNA-binding proteins, signaling proteins, and proteins involved in transcription (1, 2, 8).

Over 25 years ago heterogeneous nuclear ribonucleoproteins (hnRNPs)[1] were found to contain the majority of asymmetric dimethylarginine in HeLa cell nuclei (9). Subsequent studies of hnRNPs and related messenger RNA (mRNA)-binding proteins have revealed an intricate and evolving picture of nuclear mRNA metabolism from transcription to processing to nuclear export (10). Methylation has been implicated in the movement of hnRNP proteins across the nuclear envelope. In mammalian cells, arginine methylation has been linked to nucleocytoplasmic distribution of hnRNPA2 (11). In yeast, deletion of the predominant arginine methyltransferase, termed Hmt1 or Rmt1, inhibits nuclear export of hnRNP-like proteins (12, 13). The molecular interactions underlying these effects of arginine methylation on protein transport, however, remain to be elucidated. The yeast hnRNP-like protein Npl3, a known Hmt1 substrate (14, 15), provides an excellent system for exploring these mechanisms, because of its extensive arginine-glycine-rich domain.

Npl3 is a major yeast mRNA-binding protein that shuttles between the nucleus and the cytoplasm (16, 17). Although it is predominantly nuclear at steady state, Npl3 has been implicated in processes in both compartments, from linking transcription and mRNA export (18, 19) to acting as a translational repressor (20). Npl3 contains two central RNA-recognition motifs (RRMs) and a C-terminal domain rich in arginine (R) and glycine (G), including 15 RGG tripeptides that are likely targets for arginine methylation (21). Whereas a number of mutations within the RRMs of Npl3 block mRNA export (22), the C terminus plays a role in the nucleocytoplasmic transport of Npl3 (17, 23). The initial discovery of a genetic interaction between the temperature-sensitive *npl3-1* allele and a null

* This work was supported by Grants MCB-0235590 (to A. E. M.) and MRI-0116416 (to E. A. S.) from the National Science Foundation. The costs of publication of this article were defrayed in part by the payment of page charges. This article must therefore be hereby marked "*advertisement*" in accordance with 18 U.S.C. Section 1734 solely to indicate this fact.

[S] The on-line version of this article (available at http://www.jbc.org) contains Supplemental Data.

‡ To whom correspondence should be addressed: Dept. of Biology, 6500 College Station, Bowdoin College, Brunswick, ME 04011. Tel.: 207-798-7109; Fax: 207-725-3405; E-mail: amcbride@bowdoin.edu.

§ Supported in part by James Stacy Coles and American Society for Microbiology Undergraduate Research Fellowships.

[1] The abbreviations used are: hnRNP, heterogeneous nuclear ribonucleoprotein; CBC, cap binding complex; Cbp80, cap-binding protein, 80 kDa; DHB, 2,5-dihydroxybenzoic acid; DMA, dimethylamine; FOA, 5-fluoroorotic acid; FTMS, Fourier transform mass spectrometry; HPA, 3-hydroxypicolinic acid; inCAS, internal calibration on adjacent samples; MALDI, matrix-assisted laser desorption/ionization; PAD, protein arginine deiminase; PrA, protein A; RRM, RNA-recognition motif; TREX, transcription-export.

TABLE I
Yeast strains used in this study

Strain	Genotype	Source
nup49–313	*MATα nup49::TRP1 ade2 ade3 ura3 leu2 his3 + pUN100-nup49ts-LEU2*	(62)
PSY865	*MATα hmt1Δ::HIS3 ade2 ade8 ura3 leu2 his3 lys1*	(14)
PSY867	*MATa ade2 ade8 ura3 leu2 his3 lys1*	(14)
PSY814	*MATα npl3Δ::HIS3 ade2 ade8 can1 ura3 leu2 his3 lys1 trp1 +YCp50-NPL3–3*	(63)
PSY1096	*MATa hmt1Δ::HIS3 nup49::TRP1 ade2 ade8 ura3 leu2 lys + pUN100-nup49ts-LEU2*	(12)
PSY1943	*MATa npl3Δ::HIS3 hmt1Δ::HIS3 ade2 ade8 ura3 leu2 his3 lys1 + YCp50-NPL3–3*	(12)
PSY3210	*MATa THO2–9xmyc:TRP1 ura3 leu2 his3 lys1 trp1*	(19)
PSY3211	*MATα hmt1Δ::HIS3 THO2–9xmyc:TRP1 ura3 lys1*	(19)
YAM159	*MATa cbp80Δ::HIS3 ura3 ade2 ade8 leu2 his3*	This study
YAM505	*MATa npl3Δ::HIS3 cbp80Δ::HIS3 ade2 ade8 ura3 leu2 lys1 trp1+YCp50-NPL3–3*	This study
YAM533	*MATα hmt1Δ::HIS3 NPL3-myc:URA3 ade2 ade8 ura3 leu2 his3 lys1*	This study
YAM534	*MATα hmt1Δ::HIS3 npl3-RK1–15-myc:URA3 ade2 ade8 ura3 leu2 his3 lys1*	This study
YAM535	*MATa NPL3-myc:URA3 ade2 ade8 ura3 leu2 his3 lys1*	This study
YAM536	*MATa npl3-RK1–15-myc:URA3 ade2 ade8 ura3 leu2 his3 lys1*	This study
YAM537	*MATa THO2–9xmyc:TRP1 NPL3:URA3 ura3 leu2 his3 lys1 trp1*	This study
YAM538	*MATa THO2–9xmyc:TRP1 npl3-RK1–15:URA3 ura3 leu2 his3 lys1 trp1*	This study
YAM539	*MATα hmt1Δ::HIS3 THO2–9xmyc:TRP1 NPL3:URA3 ura3 lys1*	This study
YAM540	*MATα hmt1Δ::HIS3 THO2–9xmyc:TRP1 npl3-RK1–15:URA3 ura3 lys1*	This study
YAM569	*MATα npl3Δ::HIS3 ade2 ade8 can1 ura3 leu2 his3 lys1 trp1* + pPS2389	This study
YAM570	*MATa npl3Δ::HIS3 hmt1Δ::HIS3 ade2 ade8 ura3 leu2 his3 lys1* + pPS2389	This study

allele of *HMT1* (14), led to experiments showing that Hmt1 facilitates nuclear export of Npl3 (12). In addition, the interaction of Npl3 with two nuclear proteins, Npl3 itself and transcription elongation factor Tho2, is decreased by the presence of the arginine methyltransferase (19). These interactions, combined with the recruitment of both Npl3 and Hmt1 to actively transcribed genes (18, 19), suggest that Npl3 and Hmt1 may be involved in linking transcription and mRNA export.

The export of mRNA from the nucleus is a critical step in gene expression and increasing evidence points to the coordination of numerous proteins and complexes to guide a pre-mRNA from the site of its transcription to the site of translation. For example, components of the THO complex (Tho2, Hpr1, Mft1, Thp2), which is implicated in transcription elongation (24), interact with RNA-binding proteins Yra1 and Sub2 in a conserved protein complex named TREX (transcription-export), which has been linked to mRNA export (25). Like the TREX components, Npl3 interacts with numerous nuclear proteins. In addition to self-associating and interacting with Tho2 in the absence of methylation, Npl3 isolated from wild-type cells co-purifies with the nuclear cap binding complex (CBC; Ref. 26), RNA polymerase II (18), 3′-end processing factor Hrp1 (27), and a number of other proteins involved in mRNA metabolism (28). Interestingly, the nuclear export of Hrp1 was recently shown to depend on the methylation of Npl3 (27). With a plethora of factors influencing mRNA export, a key question remains: how are intermolecular interactions controlled over the lifetime of an mRNA, first in the formation of appropriate mRNP complexes at the site of transcription and then in the remodeling of these complexes to facilitate mRNA processing and export.

Initial studies investigating the role of Npl3 arginine methylation compared cells with wild-type *HMT1* to cells either lacking *HMT1* or expressing an inactive enzyme (12, 19, 29). The intriguing phenotypes seen in such studies and the numerous targets for arginine methylation raise two questions. First, are the effects of removing the methyltransferase direct, through eliminating Npl3 methylation, or indirect, through eliminating methylation of other substrates? Second, given the presence of an extensive arginine-glycine-rich domain in Npl3, is overall methylation of the domain or methylation of a subset of arginines important for protein function? We have used mass spectrometry, mutagenesis and assays for Npl3 activity, transport, and protein-protein interactions to address these questions *in vivo*.

Here we present mass spectrometric evidence for methylation of all arginines within RGG tripeptides and of two arginines in RG dipeptides, with variable levels of methylation detected for at least five locations. We present evidence that overall methylation is important for protein function through the introduction of systematic arginine-to-lysine mutations in RGG tripeptides followed by tests of Npl3 function in a yeast strain that requires Hmt1. We also describe experiments that suggest that arginine methylation has a direct effect on Npl3 export, its self-association and its interaction with Tho2, through the use of a mutant Npl3 protein with all RGG arginines changed to lysines (Npl3-RK1-15). These data support a model in which methylation directly affects Npl3 export by weakening contacts with nuclear proteins.

EXPERIMENTAL PROCEDURES

Yeast Strains and Plasmids—Yeast strains used in this study are listed in Table I. All strains were grown and genetic manipulations performed as previously described (30). YAM505 (*npl3*Δ *cbp80*Δ) was obtained by mating YAM159 (*cbp80*Δ) and PSY814 (*npl3*Δ). The strains used for mass spectrometric analysis, which express the protein A (PrA)-Npl3 fusion protein as the sole form of Npl3, were constructed by transforming the PrA-Npl3 plasmid pPS2389 into *npl3*Δ (PSY814) and *npl3*Δ*hmt1*Δ (PSY1943), respectively, and selecting for loss of the *URA3* maintenance plasmid, resulting in strains YAM569 and YAM570.

Plasmids used in this study are listed in Table II. Oligonucleotides used for plasmid construction and sequencing were synthesized at Integrated DNA Technologies, Inc. and are shown in Table III. Mutations that result in arginine-to-lysine substitutions within RGG tripeptides (RK mutations) were introduced by QuikChange mutagenesis (Stratagene). The seven oligonucleotide primer pairs that targeted RGG arginines 1–14 introduced two RK substitution mutations while the final pair (RK15, RK16) mutated the fifteenth RGG arginine. All primers also introduced silent base pair changes that resulted in restriction sites for identification of positive clones. The order of primer pairs used was RK9/10, RK7/8, RK5/6, RK 1/2, RK3a/RK4a, RK11/12, RK13/14, RK15/16. All mutations were verified after each round of mutagenesis by sequencing the 3′-end of *NPL3* (including the entire RGG coding region and 3′-untranslated region); the entire *NPL3* open reading frame was sequenced in the final *npl3-RK1-15* plasmid, pAM409. The only additional mutation detected in this region was the insertion of an extra T in a stretch of 10 T nucleotides in the 3′-untranslated region in plasmids pAM407-pAM409. Given the identical growth phenotypes conferred by pAM407 and its precursor pAM406, this insertion is likely to be silent. In addition, removal of the additional T from pAM409 through subcloning resulted in a plasmid that expressed the same levels of PrA-Npl3-RK1-15 as pAM409. The *GFP-npl3-RK15* plasmid, pAM420, was constructed by subcloning a 1-kb HindIII fragment from pAM409 into HindIII-digested pPS811.

To introduce the *npl3-RK1-15* mutant into the genome of strains

TABLE II
Plasmids used in this study

Plasmid	Features	Source
pAM399	*CEN LEU pNop-PrA-npl3-RK7–10 Amp^R*	This study
pAM400	*CEN LEU pNop-PrA-npl3-RK5–10 Amp^R*	This study
pAM402	*CEN LEU pNop-PrA-npl3-RK1–2,5–10 Amp^R*	This study
pAM404	*CEN LEU pNop-PrA-npl3-RK5–12 Amp^R*	This study
pAM405	*CEN LEU pNop-PrA-npl3-RK1–10 Amp^R*	This study
pAM406	*CEN LEU pNop-PrA-npl3-RK5–14 Amp^R*	This study
pAM407	*CEN LEU pNop-PrA-npl3-RK1–12 Amp^R*	This study
pAM408	*CEN LEU pNop-PrA-npl3-RK1–14 Amp^R*	This study
pAM409	*CEN LEU pNop-PrA-npl3-RK1–15 Amp^R*	This study
pAM420	*2μ URA3 pGal GFP-npl3-RK1–15 Amp^R*	This study
pAM421	*URA3 NPL3 integrating Amp^R*	This study
pAM422	*URA3 npl3-RK1–15 integrating Amp^R*	This study
pAM423	*URA3 NPL3-myc integrating Amp^R*	This study
pAM424	*URA3 npl3-RK1–15-myc integrating Amp^R*	This study
pAM431	*CEN LEU pNop-PrA-npl3-RK1–6 Amp^R*	This study
pNOPPATA	*CEN LEU pNop-PrA Amp^R vector*	(36)
pPS430	*CEN LEU pGal NPL3-myc*	(17)
pPS811	*2μ URA3 pGal GFP-NPL3 Amp^R*	(22)
pPS2389	*CEN LEU pNop-PrA-NPL3 Amp^R*	(19)
pRS306	*URA3 Amp^R vector*	(32)

TABLE III
Oligonucleotides used in this study

Introduced(+) or deleted (−) restriction sites are underlined and boldface indicating nucleotide differences from wild-type *NPL3*.

Oligo	Sequence (5′-3′)	Site/mutation
AM215	ATAGGGCGAATTGGAGCTCC	
AM216	CCTGCCCGTATGTTGAAGAGG	
RK1	CCAATCAGAAGATCT**T**AATA**A**AGGTGGCTTCAGAGGT**AAA**GGCGGCTTCAGAGG	BglII(+)/R284K, R290K
RK2	CCTCTGAAGCCGCC**TTT**ACCTCTGAAGCCACCT**T**TATT**A**GATCTTCTGATTGG	BglII(+)/R284K, R290K
RK3a	GGT**AAA**GGCGGCTTCA**A**AGGCGGCTTTAAAGGTGGCTTTAAAGG	DraI (+)/R294K, R298K
RK4a	CCTTTAAAGCCACCTTTAAAGCCGCCT**T**TGAAGCCGCC**TTT**ACC	DraI (+)/R294K, R298K
RK5	CAGAGGTGGCTTTAAAGGCGGTTTCTCCA**A**AGGCGGCTTCGG	DraI (+)/R302K, R307K
RK6	CCGAAGCCGCCTTTGGAGAAACCGCCTTTAAAGCCACCTCTG	DraI (+)/R302K, R307K
RK7	CGGTGGCCCCA**A**AGGTGGATTTGG**C**GGTCC**G**AAAGGTGGTTACGG	RsrII (+)/R314K, R321K
RK8	CCGTAACCACCTTT**C**GGACC**G**CCAAATCCACCTTTGGGGCCACCG	RsrII (+)/R314K, R321K
RK9	CGGTGGCTATTC**G**AAAGGTGGCTACGGTGGCTACTCCA**A**AGGCGGATATGG	BstBI(+)/R329K, R337K
RK10	CCATATCCGCCTTTGGAGTAGCCACCGTAGCCACCTT**T**C**G**AATAGCCACCG	BstBI(+)/R329K, R337K
RK11	CGGATATGGTGGTTC**G**AAAGGTGGTTACGATAGTCCTA**A**AGGTGGTTACG	BstBI(+)/R344K, R351K
RK12	CGTAACCACCTTTAGGACTATCGTAACCACCTT**T**C**G**AA**A**CCACCATATCCG	BstBI(+)/R344K, R351K
RK13	GGTTACGATAGTCCAAA**A**AGGTGGTTATTC**G**AA**A**AGGTGGCTATGGTGG	BstBI(+)/R358K, R363K
RK14	CCACCATAGCCACCTT**T**TC**G**AATAACCACCTTT**T**TGGACTATCGTAACC	BstBI(+)/R358K, R363K
RK15	GTAGCTACGGTGGTTC**G**AAAGGTGGTTATGATGG	BstBI(+)/R384K
RK16	CCATCATAACCACCTT**T**C**G**AACCACCGTAGCTAC	BstBI(+)/R384K

containing Myc-tagged Tho2, plasmid pAM422 was constructed by ligating the 798-bp KpnI-BamHI fragment from pAM420 into KpnI-BamHI-digested pRS306. This plasmid, containing the last 175 codons of the *NPL3* open reading frame, was linearized by HindIII digestion and transformed into PSY3210 and PSY3211. Ura+ colonies (YAM538 and YAM540) were tested for proper integration by PCR and sequencing. DNA sequencing was performed either at the University of Maine at Orono DNA sequencing facility or GeneGateway. Similarly, the KpnI-BamHI fragment from pPS2389 was subcloned into pRS306 (resulting in pAM421), linearized with HindIII, and integrated into Myc-tagged *THO2* strains to produce wild-type *NPL3* control strains YAM537 and YAM539. Genomic Myc-tagged *NPL3* and *npl3-RK1-15* strains (YAM533-536) were produced by the same strategy with integrating plasmids pAM423 and pAM424. These plasmids were constructed by ligating the 481-bp KpnI-NsiI fragment from pPS2389 or pAM420 and the ~300-bp NsiI-BamHI fragment from pPS430 (which contains a Myc tag inserted into the PmlI site at the 3′-end of the *NPL3* open reading frame; (17)) into KpnI-BamHI-digested pRS306.

Npl3 Purification for Mass Spectrometry—PrA-Npl3 was purified from *HMT1* and *hmt1*Δ cells according to published protocols (31). In brief, spheroplasts were prepared from either wild-type (YAM569) or *hmt1*Δ (YAM570) cells expressing PrA-Npl3, stored at −20 °C overnight and lysed by Dounce homogenization in the presence of protease inhibitors (1 mM phenylmethylsulfonyl fluoride and 2.5 μg/ml each of pepstatin, leupeptin, antipain, and chymostatin). To affinity purify PrA-Npl3, IgG-Sepharose beads (Amersham Biosciences) were incubated with clarified lysates at 4 °C for 1.5–2 h and, after extensive washing, Npl3 was eluted using the Tobacco Etch Virus (TEV) protease or PrA-Npl3 was eluted with acetic acid. Npl3 protein was concentrated by trichloroacetic acid precipitation (15%, v/v), resolved by SDS-PAGE and observed by Coomassie Brilliant Blue or zinc staining (Bio-Rad zinc stain kit).

Proteolytic Digests and MALDI-FTMS Analysis—PrA-Npl3 or Npl3 was excised from gels, destained with 50% methanol, 5% acetic acid (Coomassie Blue stain) or Bio-Rad zinc destain solution (according to the manufacturer's instructions) prior to proteolytic digestion. In-gel trypsin digests were performed according to the UCSF in-gel digest procedure[2] using 12.5 ng/μl trypsin (Sigma) in 25 mM ammonium carbonate. Chymotryptic digests of purified protein (in-gel) or tryptic fragments were performed in 25 mM ammonium carbonate (pH ~7.8) or in 100 mM Tris-HCl/10 mM $CaCl_2$ with a 1:20 to 1:200 chymotrypsin (Sigma) to substrate ratio. Reactions were stopped by boiling digests or adding formic acid to a final total volume of 5%. Digests were incubated at 30 °C or 37 °C overnight. After incubation, each digest solution was removed, and the remaining peptides extracted with 50% acetonitrile, 5% formic acid. Digest solutions and extracts were pooled, lyophilized, and stored at −20 °C. Some digests were further purified with C_{18} Zip Tips® (Millipore).

For mass spectrometric analysis, dried peptides were diluted in 0.1% trifluoroacetic acid, 50% acetonitrile and loaded onto a MALDI probe tip with an equal volume of 2,5-dihydroxybenzoic acid (DHB) matrix (1 M in 50% acetonitrile, 0.05% trifluoroacetic acid) or 3-hydroxypicolinic acid (HPA) matrix (0.5 M in 50% acetonitrile, 0.1% trifluoroacetic acid). Some DHB matrix solutions also contained 0.5 M fructose or fucose. Samples

[2] UCSF Mass Spectrometry Facility (2004) UCSF in-gel digest procedure. URL: donatello.ucsf.edu/ingel.html (accessed 7/27/2004).

TABLE IV

Summary of peptide masses detected in the in-gel tryptic digest of Npl3 using MALDI-FTMS

The peptide peaks attributed to the sequence where modifications were detected are shown; complete peak list is available as Supplementary Data. DHB was used as the MALDI matrix unless otherwise noted. Monoisotopic masses, $[M+H]^+$ or fragment, are shown. Dimethylated arginines are shown in bold and underlined; monomethylarginines are underlined; modifications that cannot be localized to one residue are in italics.

Observed mass	Predicted mass	Error	Residue numbers	Peptide sequence	No. CH_3	Notes[a]
Da	*Da*	*ppm*				
905.4843	905.4840	0.4	258–264	(R)LNNIEFR	0	
860.4863	860.4836	3.1	265–272	(R)GSVITVER	0	
693.4055	693.4042	1.8	275–280	(D)NPPPIR	0	3
821.4419	821.4377	5.1	282–288	(R)SN*R*GGF*R*	2	5
776.3902	776.3798	0.7	282–388	(R)SN*R*GGF*R*	2	1,5
1351.7370	1351.7342	2.1	282–293	(R)SN**R**GGF**R**G**R**GGF	6	
1306.6805	1306.6763	3.2	282–293	(R)SN**R**GGF**R**G**R**GGF	6	1
2687.4612	2687.4654	−1.6	282–305	(R)SN**R**GGF**R**G**R**GGF**R**GGF**R**GGF**R**GGF	12	2
2642.4166	2642.4076	3.4	282–305	(R)SN**R**GGF**R**G**R**GGF**R**GGF**R**GGF**R**GGF	12	1
2041.1485	2041.1467	0.9	285–302	(R)GGF**R**G**R**GGF**R**GGF**R**GGF**R**	10	2
1996.0838	1996.0889	−2.5	285–302	(R)GGF**R**G**R**GGF**R**GGF**R**GGF**R**	10	1
1354.7502	1354.7491	0.8	291–302	(R)GGF**R**GGF**R**GGF**R**	6	
1309.6925	1309.6912	1.0	291–302	(R)GGF**R**GGF**R**GGF**R**	6	1
2157.0778	2157.0737	1.9	308–329	(R)GGFGGP**R**GGFGGP**R**GGYGGYS**R**	6	
2112.0145	2112.0158	−0.6	308–329	(R)GGFGGP**R**GGFGGP**R**GGYGGYS**R**	6	1
844.3974	844.3948	3.1	322–329,330–337	(R)GGYGGYS**R**	2	
359.2031	359.2037	−1.8	349–351,356–358	(D)SPR	0	
589.3096	589.3093	0.6	373–377,394–398	(D)YGPPR	0	3
1085.4672	1085.4647	2.4	378–388	(R)GSYGGS**R**GGYD	2	4
329.1929	329.1932	−0.9	388–391	(D)GPR	0	3

[a] Notes: 1, peptide with loss of $NH(CH_3)_2$ (DMA); 2, HPA, not DHB, used as matrix; 3, cleavage C-terminal to aspartate; 4, cleavage C-terminal to aspartate with loss of H_2O; 5, one dimethylated residue at either Arg^{284}or Arg^{288}.

were analyzed using a HiResMALDI Fourier transform mass spectrometer (IonSpec, Lake Forest, CA) with a Cryomagnetics (Oak Ridge, TN) 4.7 Tesla actively shielded superconducting magnet using conditions that have been described previously (33). Samples were calibrated by internal calibration techniques using polypropylene glycol 725 and 2000 (Sigma Aldrich), using a modified version (33) of the internal calibration on adjacent samples (InCAS) technique (34).

The high resolution and internal calibration techniques permitted analysis of peptide methylation using single or multiple shifts of 14.01565 (monomethylation) or 28.03130 (dimethylation) mass units with respect to peaks in the spectrum of the unmethylated digested protein, or with respect to predicted peptide masses. The unique loss of dimethylamine (45.05785 Da) provided confirmation for an asymmetrically dimethylated arginine residue. The matrix HPA reduced metastable decay, and samples were analyzed using both matrices. Data were analyzed using peptide masses predicted using Protein Prospector MS-Digest (35), with exact mass calculations made using the IonSpec software and Microsoft Excel.

*Functional Analysis of Mutant Npl3 Proteins—npl3*Δ (PSY814) and *npl3*Δ*cbp80*Δ (YAM505) strains were transformed with the indicated PrA-Npl3 plasmids or with the pNOPPATA PrA vector plasmid. Transformants were grown overnight in Leu- medium and then cells collected, washed, counted, and a 10-fold serial dilution series was prepared from 10^6 cells/4 μl to 10^1 cells/4 μl. Dilutions were plated (4 μl) on Leu-Ura- plates to confirm viable cell numbers and on Leu- plates containing FOA to determine Npl3 function.

Fluorescence Microscopy—Nuclear export assays were performed as described by Lee *et al.* (1996). Protein localization was determined by fluorescence microscopy (Olympus BX51, GFP filter), and images were captured with a Magnafire digital camera and software (Olympus). The same exposure times were used for all samples.

Analysis of Protein-Protein Interactions—Protein interaction studies were performed essentially as described previously (19). To test Npl3-Tho2 interactions, cells expressing Tho2-Myc were lysed in PBSM (137 mM NaCl, 1.76 mM KH_2PO_4, 5.4 mM Na_2HPO_4, 5.7 mM KCl, 2.5 mM $MgCl_2$, 0.1% Triton X-100, pH 7.2) with protease inhibitors (as described in Npl3 purification). Tho2-Myc and associated proteins were purified from lysates using agarose-conjugated anti-Myc antiserum (A-14; Santa Cruz, sc-789) and eluted in Laemmli sample buffer. For Npl3 self-association studies, cells expressing PrA-Npl3, and Npl3-Myc were lysed with glass beads in PrA lysis buffer (150 mM KCl, 5 mM $MgCl_2$, 20 mM Tris-HCl, pH 8.0, 0.5% Triton X-100) supplemented with protease inhibitors. Lysates were normalized to 6 mg/ml total protein and incubated with 40 μl of IgG Sepharose beads (Amersham Biosciences). After incubation and extensive washing, PrA-Npl3 and associated proteins were eluted with 3 M $MgCl_2$ (in 50 mM Tris-HCl, pH 7.4, 0.05% Triton X-100), precipitated using 10% trifluoroacetic acid with 10 μg of insulin as carrier,[3] and resuspended in Laemmli sample buffer. Following SDS-PAGE and transfer to nitrocellulose by standard methods, immunoblots were probed with a polyclonal anti-Npl3 antiserum (1:5000) (37) or a polyclonal Myc antiserum (Santa Cruz Biotechnology, sc-789; 1:1000–1:2000), which allows visualization of PrA-Npl3 as well as Myc-tagged proteins. All proteins were visualized by enhanced chemiluminescence (Amersham Biosciences).

RESULTS

Identification of Methylated Arginines in Npl3—To investigate the molecular effects of arginine methylation on Npl3 function *in vivo*, it was necessary to identify those residues that are modified. Methylated and unmethylated Npl3 proteins were purified from *HMT1* (YAM569) and *hmt1*Δ (YAM570) lysates, respectively, and analyzed following electrophoretic separation and in-gel protease digestion by MALDI-FTMS. FTMS is a high-resolution mass spectrometric technique that provides excellent mass accuracy (38).

Enzymatic digestions were performed with trypsin and chymotrypsin to increase sequence coverage. The most relevant mass spectral data for peptides from the C-terminal region of methylated Npl3 are reported in Tables IV and V. Complete peak analysis and representative mass spectra for Npl3 isolated from *HMT1* and *hmt1*Δ cells can be found as supplemental data (JBC online). The data include peaks resulting from the loss of dimethylamine (DMA) from asymmetrically dimethylated arginine residues (39–41) and cleavages at aspartate residues (Asp-Xxx cleavage) (42, 43), which result from gas phase metastable decay on vacuum MALDI-FTMS instruments (33). Sequence coverage for the full methylated protein (74%) is summarized in Fig. 1, and details regarding the C-terminal RGG-rich region are described below.

The data shown in Tables IV and V and summarized in Fig. 1 provide direct evidence for dimethylation of 12 of 15 arginines in RGG tripeptides and indirect evidence for dimethylation of the other RGG motif arginines. In addition, these data provide evidence for variable levels of methylation for argin-

[3] Coachman, K., Warfield, L., and Hahn, S. (2002) trichloroacetic acid protein precipitation. URL:www.fhcrc.org/labs/hahn/methods/biochem_meth/tca_ppt.html (accessed 3/25/2005).

TABLE V

Summary of peptide masses detected in the in-gel chymotryptic digest of Npl3 using MALDI-FTMS

The peptide peaks attributed to the sequence where modifications were detected are shown; complete peak list available as Supplementary Data. DHB was used as the MALDI matrix unless otherwise noted. Monoisotopic masses, $[M+H]^+$ or fragment, are shown. Dimethylated arginines are shown in bold and underlined; monomethylarginines are underlined; modifications that cannot be localized to one residue are in italics; s indicates the phosphorylated serine. When more than one level of methylation was detected, the masses and number of methyl groups for the most intense peak are shown and the number of methyl groups for other peaks are shown in parentheses (see Supplementary Mass Spectral Data).

Observed mass	Predicted mass	Error	Residue numbers	Peptide sequence	No. CH_3	Notes[a]
Da	*Da*	*ppm*				
842.4724	842.4730	−0.8	264–271	(F)RGSVITVE	0	4
705.4163	705.4155	−1.1	288–293	(F)**R**G**R**GGF	4	1
464.2628	464.2616	2.6	294–297	(F)**R**GGF	2	
			298–301			
			302–305			
551.2926	551.2936	−1.8	306–310	(F)S**R**GGF	2	
1207.6325	1207.6331	0.5	306–317	(F)S**R**GGFGGP**R**GGF	4	1
675.3573	675.3573	0.03	311–317	(F)GGP**R**GGF	2	
1347.6949	1347.6916	−2.4	311–324	(F)GGP**R**GGFGGP**R**GGY	4	1
691.3516	691.3522	−0.01	318–324	(F)GGP**R**GGY	2	
968.4571	968.4585	1.4	318–327	(F)GGP**R**GGYGGY	2	
1121.5021	1121.5011	−0.9	325–335	(Y)GGYS**R**GGYGGY	2	2
844.3950	844.3948	−0.2	325–332	(Y)GGYS**R**GGY	2	
			328–335	(Y)S**R**GGYGGY		
			333–340	(Y)GGYS**R**GGY		
567.2871	567.2885	−2.5	328–332	(Y)S**R**GGY	2	
			336–340			
			362–366			
681.3291	681.3315	3.5	341–347	(Y)GGS**R**GGY	2 (0)	
			381–387			
1385.6252	1385.6193	−4.3	341–354	(Y)GGS*R*GGYDSP*R*GGY	0 (1,2)	2, 5
1483.6533	1483.6561	1.9	348–361	(Y)DSPRGGYDSPRGGY	0 (1,2)	2
778.3490	778.3478	−1.4	341–348	(Y)GGS**R**GGYD	2 (0,1)	4; isobaric with unmethylated 367–373
			381–388			
733.3265	733.3264	−0.2	348–354	(Y)DSP**R**GGY	0 (0,2)	6
			355–361			
664.3412	664.341	0.2	349–354	(D)SP**R**GGY	2 (0,1)	3
			356–361			
1326.620	1326.6185	−1.2	362–373	(Y)S**R**GGYGGPRNDY	2	2
597.2740	597.2440	−0.1	367–372	(Y)GGPRND	0	4
1492.6943	1492.6928	−1.0	367–380	(Y)GGPRNDYGPPRGSY	0	Isobaric with 333–347 with 3 CH_3
1506.7137	1506.7084	−3.5	367–380	(Y)GGPRNDYGPP*R*GSY	1	Isobaric with 333–347 with 4 CH_3
1520.7291	1520.7241	−3.3	367–380	(Y)GGPRNDYGPP**R**GSY	2	
924.4563	924.4574	1.2	373–380	(D)YGPP**R**GSY	2 (0,1)	3
2198.0075	2198.0001	−2.9	381–401	(Y)GGS**R**GGYDGPRGDYGPPRDAY	2 (0,1)	
1535.6877	1535.6874	−0.2	388–401	(Y)DGPRGDYGPPRDAY	0	2
1677.8293	1677.8293	−0.02	402–414	(Y)RTRDAPRERsPTR	0	2
1579.8520	1579.8524	−0.2	402–414	(Y)RTRDAPRERsPTR	0	2, 7

[a] Notes: 1, peptide with loss of $NH(CH_3)_2$ (DMA); 2, HPA, not DHB,used as matrix; 3, cleavage C-terminal to aspartate; 4, cleavage C-terminal to aspartate with loss of H_2O; 5, modification cannot be localized to one residue; 6, peptide with loss of H_2O; 7, peptide with loss of H_3PO_4.

1 MSEAQETHVE QLPESVVDAP VEEQHQEPPQ APDAPQEPQV PQESAPQESA

51 PQEPPAPQEQ NDVPPPSNAP IYEGEESHSV QDYQEAHQHH QPPEPQPYYP

101 PPPPGEHMHG RPPMHHRQEG ELSNTRLFVR PFPLDVQESE LNEIFGPFGP

151 MKEVKILNGF AFVEFEEAES AAKAIEEVHG KSFANQPLEV VYSKLPAKRY

201 RITMKNLPEG CSWQDLKDLA RENSLETTFS SVNTRDFDGT GALEFPSEEI

251 LVEALERLNN IEFRGSVITV ERDDNPPPIR RSNRGGFRGR GGFRGGFRGG

301 FRGGFSRGGF GGPRGGFGGP RGGYGGYSRG GYGGYSRGGY GGSRGGYDSP

351 RGGYDSPRGG YSRGGYGGPR NDYGPPRGSY GGSRGGYDGP RGDYGPPRDA

401 YRTRDAPRER SPTR

FIG. 1. **Location of methylarginine residues in Npl3.** The amino acid sequence of Npl3 is shown. Residues detected in tryptic or chymotryptic peptides of methylated Npl3 are *underlined once*, and those detected in both digests are *underlined twice*. Dimethylarginine residues are marked with a *filled circle*; residues that are seen to be dimethylated with additional evidence for possible monomethylation or lack of methylation are marked with *open circles*.

ines in both RGG and RG contexts. There was no evidence for methylation of other arginine residues within or outside the RGG domain of Npl3 isolated from wild-type cells. The lack of evidence for methylarginine residues in Npl3 isolated from *hmt1*Δ cells (see Supplemental Data) also suggests that neither of the other two known *Saccharomyces cerevisiae* protein arginine methyltransferases, Hsl7 (44) and Rmt2 (45), methylates Npl3 *in vivo*.

Asymmetrical dimethylation of arginines Arg^{284} through Arg^{329} is strongly supported by the detection of 14 peptides, with associated losses of DMA, in the tryptic and chymotryptic digests (Tables IV and V). Two of the detected peptides show

masses indicating cleavage C-terminal to phenylalanine (Table IV). Although trypsin has stringent specificity for arginine and lysine residues (46), the low mass measurement errors indicate that these peaks are correctly assigned. We also detected a peak at *m/z* 821.44 in the tryptic digest, with a DMA loss at *m/z* 776.39. These peaks likely specify a peptide sequence with only one arginine residue, Arg^{284} or Arg^{288}, which is dimethylated. In contrast with evidence for this single peptide with one unmethylated arginine, four Arg^{284}/Arg^{288} peptides in the tryptic and chymotryptic digests showed evidence for dimethylation of both residues. In summary, we have strong support for eight consecutive RGG motif arginines (Arg^{290}-Arg^{329}) that are exclusively dimethylated (no evidence for mono- or nonmethylation). Additionally, residues Arg^{284} and Arg^{288} are dimethylated, with the detection of one peptide providing evidence for nonmethylation of either Arg^{284} or Arg^{288}.

Peaks from the chymotryptic, not tryptic, digest provided the most informative peptide peaks for arginines beginning with Arg^{344} and extending through to the C terminus of the sequence (Table V). Our data provide strong evidence for the methylation state of arginines beginning at Arg^{363} and proceeding through to the C terminus. Dimethylation of arginine Arg^{363} is supported by the detection of a peptide at *m/z* 1326.62. The site of dimethylation is localized to Arg^{363} by the detection *m/z* 597.24, which is found as a nonmethylated peak. The data support non-, mono-, and dimethylation of arginine Arg^{377}, which is located in an RG motif. The most intense peaks, which correspond to the nonmethylated product, appear at *m/z* 1492.69 and 896.43. Mono- and dimethylation are indicated by lower intensity peaks at *m/z* 1506.71 and 1520.73. While the *m/z* 1506.71 peak is not unique (isobaric with the chymotryptic peptide for residues 333–347), the *m/z* 1520.73 peak and *m/z* 910.44 and 924.46 fragments uniquely support mono- and dimethylation at this residue. Additionally, associated with the *m/z* 1506.71 and 1520.73 peaks are losses of H_2O and NH_3 that parallel those observed for *m/z* 1492.69 when it was detected in the nonmethylated Npl3 digest (see Supplemental Data), reflecting losses from aspartate and asparagines residues. Collectively, these data support our conclusion that Arg^{377} is present in unmethylated, monomethylated, and dimethylated forms. The intensities of the unmethylated peptides peaks (*m/z* 1492.69 and 896.43) suggest that the RG motif Arg^{377} is found largely in an unmethylated state.

The most intense peak attributed to the RGG motif arginine Arg^{384}, *m/z* 2198.00, reflects dimethylation of this residue; however, we also detect lower abundance peaks showing that this residue also appears in a mono- and nonmethylated state (Tables IV and V, and Supplemental Data). The data also provide strong support for our conclusion that the seven remaining arginine residues at the C terminus of the protein are unmodified (Tables IV and V), including an additional RG and two R*X*R arginines. Whereas methylated R*X*R motifs were found in poly(A)-binding protein II (47), none of the arginines in the three R*X*R motifs is methylated in Npl3. We also detect phosphorylation of the C terminus serine residue, in agreement with previous findings (48, 49).

Our results for arginine residues Arg^{337}, Arg^{344}, Arg^{351}, and Arg^{358} are less definitive. Dimethylation of Arg^{337} is supported by the exclusive detection of *m/z* 844.40, not *m/z* 816.36, in both the tryptic and chymotryptic digests; however, for both digests this mass reflects a redundant region of the sequence and does not uniquely specify the methylation state of Arg^{337}. Although indirect, we find no evidence to disprove the conclusion that this residue is dimethylated. For arginines Arg^{344}, Arg^{351}, and Arg^{358} we find a significant number of peaks that suggest lower and variable levels of methylation associated with these three arginines. Two longer peptides, *m/z* 1385.62 (for Arg^{344}/Arg^{351}) and *m/z* 1483.65 (for Arg^{344}/Arg^{351}) (Table V) are detected as unmodified. In addition they are found as mono- or dimethylated peptides that appear at *m/z* 1399.63 and 1413.65 (for Arg^{344}/Arg^{351}) and *m/z* 1497.67 and 1511.69 (for $Arg^{351/358}$) (Supplemental Data). A number of lower mass peaks, attributed to shorter peptides containing one arginine residue, also show variable levels of methylation. These include the dimethylated versions at *m/z* 681.33 and 778.35 (for Arg^{344}/Arg^{384}) and 664.34 (for Arg^{351}/Arg^{358}) (Table V), as well as peaks including *m/z* 733.33 (Arg^{351}/Arg^{358}) that show zero or one methyl group addition (Table V and Supplemental Data). The peak at *m/z* 359.20 (Arg^{351}/Arg^{358}) from the tryptic digest (Table IV) was found exclusively as the unmethylated version. Because of the repetitive nature of sequences in this region and isobaric masses, we cannot distinguish contributions from each residue ($Arg^{344}/Arg^{351}/Arg^{358}$). We conclude that Arg^{344}, Arg^{351}, and Arg^{358} are present in variable methylation states with evidence to suggest that di-, mono-, and unmethylated versions of these residues may be present, and use indirect evidence to support dimethylation of Arg^{337}.

In summary, the mass spectral data reveal direct evidence for dimethylation of 12–15 arginines in RGG tripeptides, and indirect support for dimethylation of an additional residue (Arg^{337}), as summarized in Fig. 1. Evidence was found suggesting variable levels of methylation for two RG dipeptides. In one case (Arg^{377}), lower abundance mono- and dimethylated peaks were localized to this residue. In the second case, dimethylation was present for all but one detected peptide, and for that instance Arg^{288} (RG) could not be distinguished from Arg^{284} as the unmodified residue. While nine consecutive N-terminal RGG motif arginines were found to be exclusively dimethylated, we found evidence for variable levels of methylation associated with four C-terminal RGG motif arginines (Arg^{344}, Arg^{351}, Arg^{358}, and Arg^{384}). For Arg^{344}, Arg^{351}, and Arg^{358} we were unable to localize the level of methylation to a specific residue because of redundant sequence masses. Additionally, there was no evidence of methylation of arginines outside the RGG domain.

Effect of Arginine-to-Lysine Mutations on Npl3 Function in Vivo—The presence of 15 RGG tripeptides within Npl3 raises the question of whether specific arginines or their methylation are important for Npl3 function or whether overall methylation of Npl3 plays a key role. With the identification of numerous methylated arginines in the C terminus of Npl3, we decided to mutate all the arginines within RGG contexts to lysines to test the effect of methylation on Npl3 function. The conservative Arg-to-Lys (RK) mutation retains the positive charge of the residue (Fig. 2*A*) while removing its ability to be targeted by the arginine methyltransferase (50). Arginines within RGG peptides have been numbered 1-15 from the N terminus to simplify mutant nomenclature (Fig. 2*B*). We created a set of 20 Npl3 mutants by adding two RK mutations at each round of mutagenesis (Fig. 2*B*). Mutations were introduced into a plasmid that expresses a functional protein A (PrA)-Npl3 fusion protein (pPS2389) to facilitate subsequent protein-protein interaction analysis (19).

RK mutants could impact protein function either due to the need for arginine at a certain position or to the importance of methylation of that residue. To distinguish between these two effects, we tested Npl3-RK mutants for function in two different strain backgrounds. Although most strains lacking HMT1 are viable, a strain in which the 80 kDa cap-binding protein gene (*CBP80*) has been deleted requires the arginine methyltransferase for growth (12). In addition, a cold-sensitive *hmt1* allele identified in the *cbp80*Δ background showed a specific

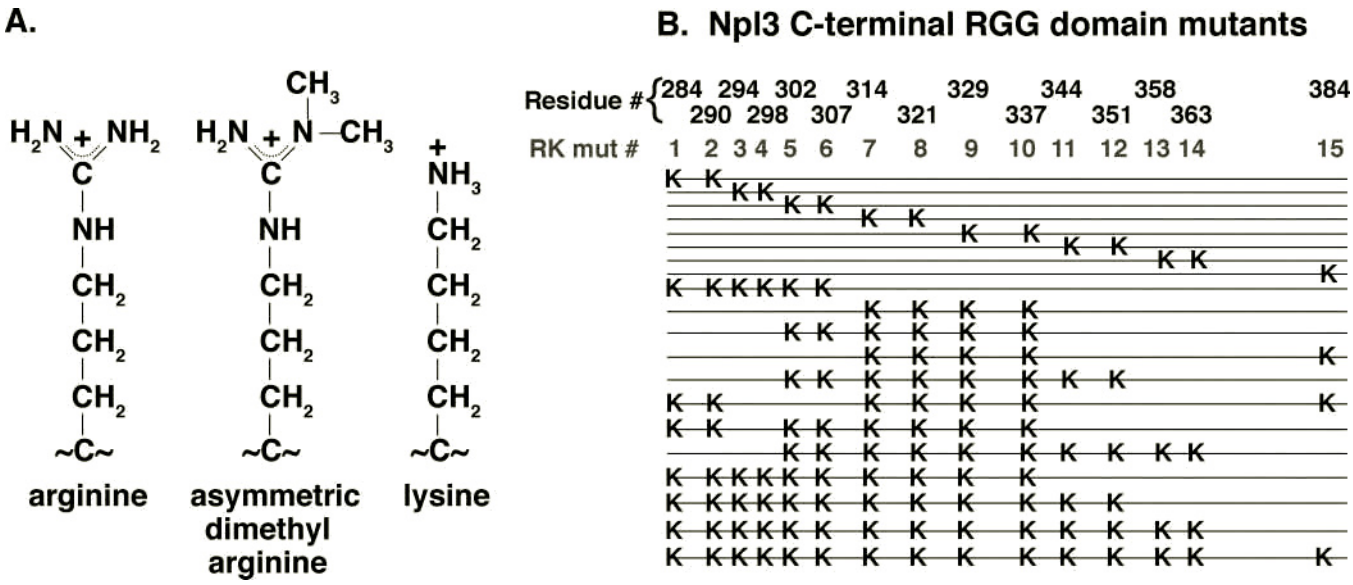

FIG. 2. **Arginine-to-lysine substitution mutations in Npl3.** *A*, structural comparison of arginine, asymmetric dimethylarginine and lysine. The peptide backbone is denoted by ~*C*~. *B*, schematic diagram of the 20 mutant Npl3 proteins. Residue numbers for the arginines mutated within RGG tripeptides are shown above the simplified numbering system. *K* denotes the arginines that have been changed to lysines in each mutant protein (*e.g.* the *top line* represents mutant Npl3-RK1–2 and the *bottom line*, mutant Npl3-RK1-15).

defect in Npl3 methylation (29). These genetic and biochemical findings suggest a complementary role for Npl3 methylation and Cbp80 in these strains. Therefore, if Npl3 methylation is important in strains lacking Cbp80, Npl3-RK mutants, which should not be methylated, would be predicted to support growth of an *npl3*Δ strain but show poorer rescue of an *npl3*Δ *cbp80*Δ strain.

Fig. 3 shows the growth of the *npl3*Δ mutant (PSY814) expressing each of the Npl3-RK mutants. The Npl3 protein with all 15 arginines within RGG peptides mutated to lysines (RK1-15) is able to support growth of *npl3*Δ at 30 °C to the same extent as wild-type Npl3, with only a slight growth defect at 20 °C and 37 °C. Thus the RK mutants are still functional. The deletion of *HMT1* does not affect the growth of strains expressing either wild-type PrA-Npl3 or PrA-Npl3-RK1-15 (data not shown), as expected. In contrast, the expression of PrA-Npl3-RK mutant proteins in the *npl3*Δ*cbp80*Δ strain (YAM505) has a significant effect on growth (Fig. 4). This effect is significantly more pronounced at low and high temperature (Fig. 4). Therefore in a background in which *HMT1* is essential, the substitution of multiple lysines for arginines at methylation sites results in a significant loss of Npl3 function.

Although mutating two neighboring or a single RGG arginine (RK1–2, RK3–4, RK5–6, RK7–8, RK9–10, RK11–12, RK13–14, and RK15) showed no effect on Npl3 protein function as assessed by growth of *npl3*Δ*cbp80*Δ cells (data not shown), increasing the number of RK mutations increased the severity of the phenotype (Fig. 4). This result suggests that cumulative methylation of Npl3 is important for protein function. When mutations in the first and second RGG arginines were added to Npl3-RK5-10, however, there was a more severe effect on growth than when either mutations in arginines 11–12 or 11–14 were added (Fig. 4, 20 °C, 37 °C). This result suggests the relative increased importance of the N-terminal RGG arginines, particularly at low temperature where the effect is most pronounced. Indeed, while PrA-Npl3-RK1–6 supports equivalent growth to PrA-Npl3-RK5–14 at 37 °C, PrA-Npl3-RK1–6 grows significantly more poorly at 20 °C (data not shown). Therefore, although the total number of arginines that can be methylated is important for Npl3 function, it appears that the N-terminal RGG arginines may play a specific role.

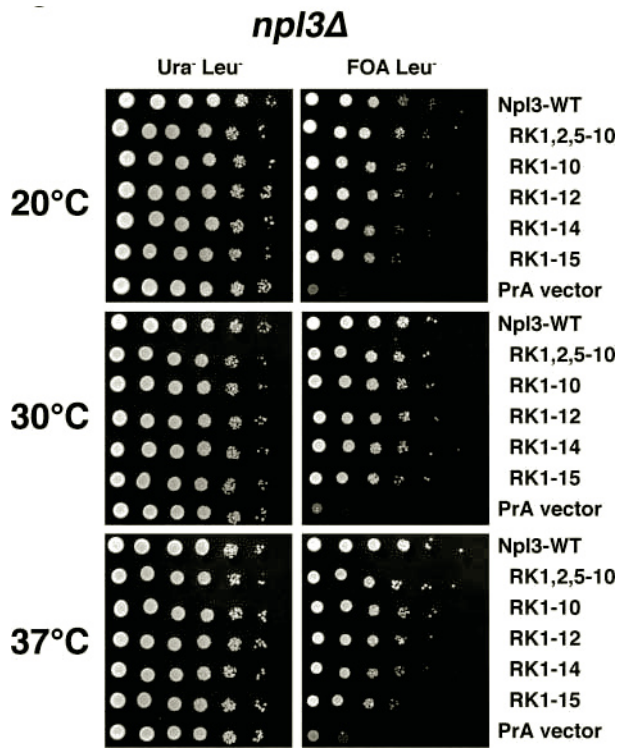

FIG. 3. **Npl3 with all RGG arginines mutated to lysines is functional.** *npl3*Δ*+NPL3 URA3* cells (PSY814) were transformed with PrA plasmids containing wild-type (*WT*) *NPL3*, mutant forms of *npl3*, or no *NPL3* (*PrA vector*). Serial 10-fold dilutions of cells were plated on Ura-Leu- media, to demonstrate equal cell numbers, and FOA medium, to test for mutant Npl3 function at the indicated temperature.

Arginine-to-Lysine Mutations Result in Methylation-independent Export of Npl3—Because the arginine methyltransferase facilitates the export of Npl3 (12), we wished to use the Npl3-RK1-15 mutant to test whether the Hmt1 effect on export was direct, because of methylation of Npl3, or indirect, through the methylation of another protein. To examine export we used an established assay in which the import of GFP-Npl3 is blocked by shifting a strain with a mutation in a nuclear pore protein

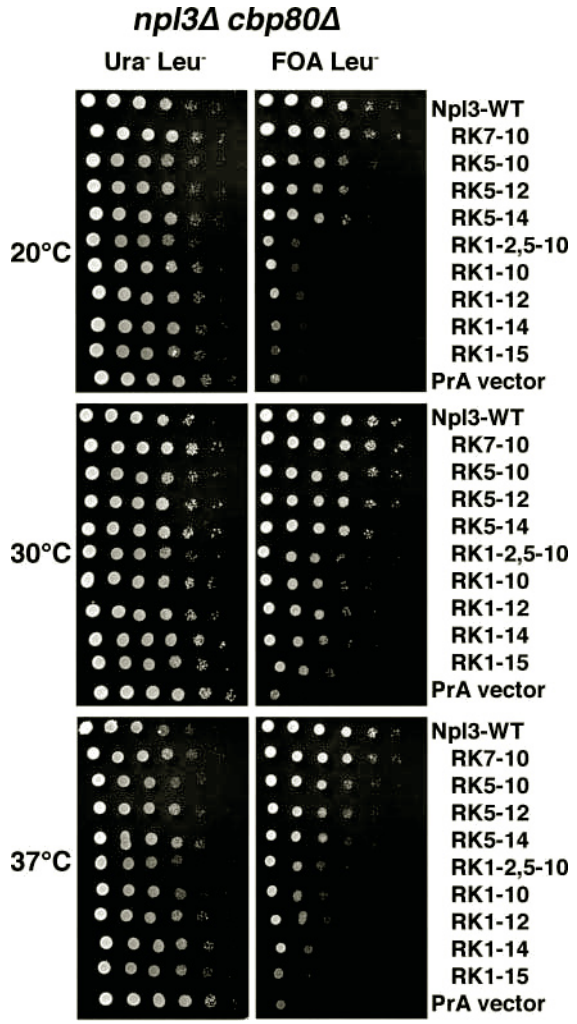

FIG. 4. **Arginine-to-lysine mutations in *NPL3* are deleterious in the absence of the 80 kDa cap-binding protein.** A strain lacking the 80-kDa cap-binding protein gene, YAM505 (*npl3*Δ*cbp80*Δ+*NPL3 URA3*), was transformed with PrA plasmids containing mutant forms of *npl3* and positive (*WT*) and negative (*PrA vector*) controls. The function of mutant Npl3 proteins was tested by a plasmid shuffle assay as described in the legend for Fig. 3.

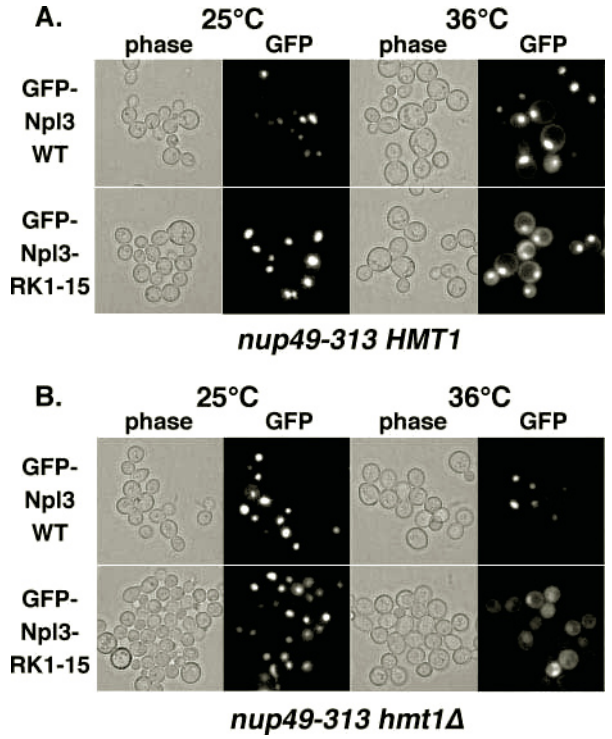

FIG. 5. **Methylation-independent nuclear export of Npl3-RK1-15.** *A*, expression of GFP-Npl3 or GFP-Npl3-RK1-15 in the *nup49-313* strain was induced for 2 h and then repressed for 2 h at 25 °C. To block Npl3 nuclear import, half of each culture was shifted to 36 °C for 5 h, and protein localization was detected by direct fluorescence microscopy. *B*, nuclear export of wild-type and mutant fusion proteins in a strain lacking the arginine methyltransferase (*nup49-313 hmt1*Δ; PSY1096) was tested as in *A*.

(*nup49-313*) to high temperature, allowing the export of GFP-Npl3, a predominantly nuclear shutting protein, to be detected by increased cytoplasmic fluorescence (22). This relocalization of wild-type GFP-Npl3 is inhibited by the deletion of *HMT1* (12).

The nuclear export of GFP-Npl3-RK1-15 in the *nup49-313* mutant with or without *HMT1* is compared with that of wild-type GFP-Npl3 in Fig. 5. Like GFP-Npl3, GFP-Npl3-RK1-15 is predominantly nuclear in wild-type and *hmt1*Δ cells at 25 °C. The cytoplasmic GFP-Npl3-RK1-15 signal at high temperature in *nup49-313* cells indicates that methylarginine residues in Npl3 are not required for its export (Fig. 5*A*). However, some cytoplasmic GFP-Npl3-RK1-15 is also seen at the non-permissive temperature in *nup49-313* lacking the methyltransferase (Fig. 5*B*), demonstrating that methylation of other proteins is not required for Npl3 export. These results concur with recently published data from Xu and Henry (27). Therefore, the methylation-independent export of GFP-Npl3-RK1-15 supports a model in which either methylation of arginine residues or substitution with lysine weakens a nuclear complex, facilitating Npl3 export.

Methylation-independent Interaction of Npl3-RK1-15 with Tho2—Our results suggest that Npl3 should interact with nuclear molecules and that these interactions should be decreased by methylation. We have previously identified two molecular partners of Npl3 with these characteristics: the transcription elongation factor Tho2 and Npl3 itself (19). To test whether the Tho2 interaction is affected by the Npl3-RK1-15 mutations, this mutant was integrated into *HMT1* and *hmt1*Δ strains expressing Myc-tagged Tho2. Following immunoprecipitation of Tho2-Myc from these strains and strains expressing wild-type Npl3, copurifying Npl3 was detected with a polyclonal Npl3 antiserum (Fig. 6). While wild-type Npl3 copurifies with Tho2-Myc from *hmt1*Δ strains (*lane 1*), the Npl3-RK1-15 mutant protein shows a reduced interaction with Tho2-Myc (*lane 2*). This reduced interaction is not caused by differential recognition by the Npl3 antiserum, which was raised against a truncated Npl3 lacking the RGG domain (37), nor is the mutant protein expressed at lower levels than the wild-type protein (Fig. 6, *lysate*). In addition, the Tho2-Myc interaction with wild-type Npl3 is not detected in *HMT1* cells whereas the reduced interaction with Npl3-RK1-15 is still observed (*lanes 3* and *4*). These results support the possibility that lysine, like dimethylarginine, loosens a nuclear Npl3 complex that contains Tho2-Myc, which could facilitate export even in the presence of the arginine methyltransferase.

RK1-15 Mutations Block Npl3-Npl3 Interactions—To test the effect of the Npl3-RK1-15 mutation on Npl3 self-association, Myc-tagged forms of the wild-type and mutant *NPL3* genes were integrated into *hmt1*Δ and *HMT1* strains and the resulting strains transformed with the PrA-Npl3 plasmids. IgG-Sepharose was then used to isolate PrA-Npl3 and associated proteins and PrA-Npl3 and Npl3-Myc were detected with a polyclonal Myc antiserum. When the RK1-15 mutations are present in both forms of Npl3, no Npl3-Npl3 interaction is

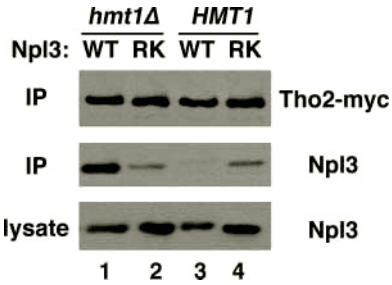

FIG. 6. **Methylation-independent interaction of Npl3-RK1-15 with transcription elongation factor Tho2.** *HMT1* and *hmt1*Δ cells expressing Myc-tagged Tho2 and either wild-type (*WT*) or RK1-15 (*RK*) Npl3 proteins from their endogenous loci were lysed, lysates were normalized for total protein and Tho2-associated proteins isolated with anti-Myc agarose beads. Bound proteins were eluted in Laemmli buffer and analyzed by anti-Myc and anti-Npl3 immunoblotting. Npl3 protein levels in lysates are also shown.

detected even in the absence of the methyltransferase (Fig. 7, *lane 2*), demonstrating the critical role of arginines in Npl3 self-association. Introducing the RK mutations into PrA-Npl3 results in a reduced interaction with wild-type Npl3-Myc in the *hmt1*Δ strain (*lane 4*), suggesting that unmethylated arginines in each monomer make important contacts for self-association. Although the interaction in the reverse orientation, between Myc-tagged Npl3-RK1-15 and PrA-Npl3 (*lane 3*), is not seen, the C-terminal placement of the Myc tag may further disrupt an interaction that involves the C terminus of the mutant protein. These data therefore suggest that Npl3 self-association and interaction with Tho2 reflect dynamic nuclear complexes that are influenced by Npl3 methylation.

DISCUSSION

Npl3 is a particularly interesting model to explore the effects of arginine methylation on protein function because of its extensive arginine-glycine-rich domain, which has 15 RGG, 3 RG, and 2 R*X*R peptides (Fig. 1). This long C-terminal domain allowed us to address the question whether overall methylation or methylation of a subset of arginines influenced protein function. Using mass spectrometry, we identified 16 arginine residues that are dimethylated *in vivo*, and one additional arginine that is likely to be dimethylated. Whereas evidence pointed to variable levels of methylation for two RG dipeptides and at least three RGG tripeptides, the vast majority of dimethylarginine in Npl3 is found in the RGG context (Fig. 1). Mutating these residues to lysine affected general Npl3 function only in a strain background that requires the methyltransferase. Whereas increasing the total number of lysine substitutions generally increased the severity of the growth phenotype, mutations in the four RGG tripeptides at the N terminus of the domain had a greater influence on Npl3 function than mutating RGGs more C-terminal (Fig. 4), suggesting a specific role for these residues.

The seven N-terminal RGG arginines are followed by phenylalanine (F) residues, including tandem RGGF repeats from Arg^{290}–Arg^{302} (RGG2–5), with an average of two residues between RGG tripeptides (Fig. 1). The next seven RGGs are all followed by tyrosine residues, with an average spacing of four residues between RGG tripeptides. Although the three-dimensional structure of Npl3 has not been determined, these results suggest that the influence of arginine methylation or lysine substitution on Npl3 structure and activity may be greater at the N terminus of this domain where the arginines are more closely spaced in the primary structure.

Lysine substitutions are commonly used both to determine sites of arginine methylation and to probe the functional significance of methylarginine residues within a protein (27, 51–54). This choice is based on 1) both lysine and arginine being long chain amino acids with a positive charge at physiological pH and 2) lysine not being a target for protein-arginine methyltransferases (50). Although methylation should not alter the positive charge of arginine, asymmetric dimethylation increases the hydrophobicity of the residue, is likely to have steric effects on inter- or intramolecular contacts and may also influence hydrogen bonding (2, 6, 55). Whereas lysine maintains a positive charge and should not incur the same steric effects that occur upon arginine methylation, this substitution could still decrease arginine-specific contacts of the protein. The challenge of using RK mutations to distinguish between direct and indirect effects of arginine methylation on protein function is to try to separate effects of loss of arginine function from loss of methylation of the arginine in question.

The ability of lysine to substitute for arginine in the C-terminal domain of Npl3 is supported by the robust growth of *npl3*Δ strains expressing the Npl3-RK1-15 mutant protein and the steady-state nuclear localization of this protein (Figs. 3 and 5). Xu and Henry have also used an elegant cloning strategy to construct an Npl3 mutant with all RGG arginines mutated to lysine (Npl3(KGG)) by introducing similar missense mutations and four fewer silent mutations (27). They detected steady-state nuclear localization of Npl3(KGG) and reported that this protein was functional and was not methylated *in vivo* (27). In their experiments, Npl3(KGG) expressed from a plasmid rescued the synthetic lethality of an *npl3-1 hmt1*Δ strain, and we have also found that Npl3-RK1-15 supports growth of an *npl3*Δ*hmt1*Δ strain (data not shown). These results were expected given the non-essential nature of HMT1 and the viability of the *npl3*Δ strain expressing Npl3-RK1-15. Because the arginine methyltransferase gene is not essential, these results do not address whether arginine methylation of Npl3 in particular has functional consequences for cell growth.

When a set of Npl3-RK mutant proteins is expressed in a strain lacking the 80-kDa cap-binding protein, however, mutant proteins with increased numbers of lysine substitutions show a more severe growth defect (Fig. 4). Because the *cbp80*Δ background requires *HMT1* for viability, these results suggest that methylation of Npl3 in particular is important in this background. Whereas the *cbp80*Δ strain that expresses Npl3-RK1-15 grows slowly at 30 °C (Fig. 4), the deletion of *HMT1* in the *cbp80*Δ background is lethal (12). This result could either reflect the importance of methylation of Arg^{288} and Arg^{377}, which are variably methylated *in vivo* and were not mutated in Npl3-RK1-15, or methylation of another protein in the *cbp80*Δ strain. Alternatively, the greater severity of the *hmt1* deletion may be explained by lysine exerting an intermediate effect, falling functionally between unmethylated and methylated arginine.

The importance of the Hmt1 arginine methyltransferase for the export of its mRNA-binding substrates Npl3, Hrp1, and Nab2 (12, 13) suggests a role for this post-translational modification in the process of directing export or remodeling nuclear complexes to facilitate export. Deletion analysis of Nab2 (56) and the identification of Npl3 protein-protein interactions that are decreased by methylation (19) pointed to the second model. Whereas Npl3 phosphorylation at a C-terminal serine plays a role in nuclear import by promoting dissociation from mRNA and binding to the Mtr10 import receptor (48, 49), *in vitro* data also suggest that Hmt1 has an indirect effect on Npl3 binding to Mtr10 (48). The identification of specific sites of methylation in Npl3 has now allowed us to test whether methylation effects on Npl3 export are direct or indirect.

Although the RGG domain of Npl3 is necessary for nuclear import (17, 23), the nuclear localization of GFP-Npl3-RK1-15 in *nup49-313* strains at 25 °C (Fig. 5) indicates that these muta-

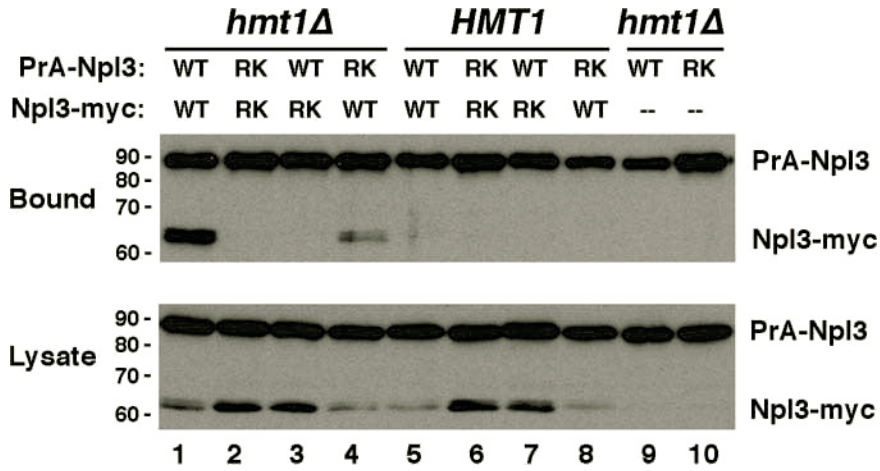

FIG. 7. **Arginine-to-lysine mutations block Npl3 self-association.** *HMT1* and *hmt1*Δ strains expressing Myc-tagged wild-type (*WT*) or RK1-15 (*RK*) Npl3 proteins from the endogenous locus were transformed with PrA-Npl3 or PrA-Npl3-RK1-15 plasmids. YAM7 (*hmt1*Δ) with an untagged genomic *NPL3* gene was used to control for PrA-Npl3 degradation (*lanes 9* and *10*). Cells were lysed, and lysates were normalized for total protein prior to isolation of PrA-Npl3-associated proteins with IgG-Sepharose beads. Bound proteins were eluted with 3 M $MgCl_2$, precipitated with trichloroacetic acid, resuspended in Laemmli buffer and analyzed by anti-Myc immunoblotting. Npl3 protein levels in lysates are also shown.

tions do not have a severe effect on Npl3 import into the nucleus. The Npl3-RK1-15 mutant protein also can exit the nucleus even in the absence of the methyltransferase, as also seen for Npl3(KGG) by Xu and Henry (27). This result suggests that, whereas methylation may block specific nuclear contacts made by arginine in Npl3, the lysine substitutions may promote export in this assay through their inability to mediate nuclear protein-protein interactions. Whereas RK mutations in Npl3 directly affect Npl3 export, similar mutations in the three RGG tripeptides in Hrp1 do not influence its export (27). Intriguingly, the expression of the Npl3(KGG) mutant protein facilitated the export of Hrp1 in the absence of Hmt1, suggesting that the methylation of Npl3 is important for the export of an interacting protein (27).

Npl3 copurifies with Hrp1 and the nuclear cap-binding complex, but these interactions are not influenced by the presence of Hmt1 (19, 26, 27). In contrast, interactions of Npl3 with Tho2 and Npl3 are affected either by the presence of the methyltransferase (19) or by the presence of RK mutations within Npl3 (Figs. 6 and 7), arguing for a direct effect of Npl3 methylation on nuclear protein complex formation. The Npl3 self-association is more severely affected by RK mutations than the Npl3-Tho2 interaction. This difference may be because of the C-terminal Myc tag used in self-association studies (see "Results"). Alternatively, different contacts may be involved in the two interactions, a likely possibility given the RNase sensitivity of the Npl3-Tho2 interaction and RNase resistance of self-association (19). Xu and Henry found that whereas *HMT1* deletion did not affect UV-cross-linking of Npl3 to bulk poly(A) RNA *in vivo*, more Npl3(KGG) than wild-type Npl3 copurified with poly(A) RNA after cross-linking (27). Therefore, even though the RK mutations may decrease protein-protein interactions that are important for the copurification of Tho2 with Npl3, the Tho2-Npl3-RK1-15 interaction may still be detected because of increased binding of the mutant Npl3 to pre-mRNA. In combination these data support a model in which arginine methylation of Npl3 specifically modulates mRNP formation by loosening contacts with nuclear proteins, thereby facilitating export. The synthetic lethality of *npl3-1* and *cbp80*Δ with *hmt1*Δ may reflect the combination of decreased binding of export-facilitating proteins to mRNA with stronger interactions of Npl3 with a specifically nuclear complex.

Chromatin immunoprecipitation experiments have also revealed interesting binding patterns for proteins involved in mRNA metabolism. Whereas Hmt1 and Npl3 are present at the promoter and toward the 5′-ends of highly transcribed genes (18, 19), polyadenylation factors bind preferentially to the 3′-end (57). TREX components are cross-linked to coding regions but binding is much lower at the promoter or downstream of polyadenylation signals (18, 25, 57). In addition, recent work has shown that mutations in Npl3 enhance transcription termination, pointing to a role for Npl3 in antagonizing mRNA 3′-end formation (58). Taken together, these results support a model in which a series of proteins associates with DNA and likely nascent mRNA at the site of transcription, with Npl3 associating near the beginning of transcription, followed by TREX components and then polyadenylation factors. By decreasing association with Tho2 and potentially other TREX proteins, methylation of Npl3 near the 5′-end of actively transcribed genes may help remodel mRNPs and thus facilitate export.

The discovery of protein-arginine deiminases (PADs) that can convert methylarginines to citrulline within histones (59, 60), raises the tantalizing possibility that arginine methylation may be reversible. Non-histone substrates of both type I and type II methyltransferases can also be targets for deimination (54, 61), but *in vitro* data suggest that arginine dimethylation inhibits deimination (60, 61). We did not detect citrulline residues within Npl3 by mass spectrometry and *S. cerevisiae* has no obvious PAD homolog. Therefore, whereas we cannot rule out the possibility that Npl3 deimination may allow increased nuclear interactions, Npl3 methylation is likely to have a more long term effect on the balance between transcriptional and export complexes.

Numerous type I arginine methyltransferase substrates are involved in mRNA transcription and export, from histones to transcription factors to hnRNPs. Therefore the various effects seen in *hmt1*Δ cells, from synthetic lethal interactions to altered mRNA binding profiles to protein export defects, likely reflect altered methylation of proteins in addition to Npl3. Nab2, Yra1, and Tho2, for example, are all targets for *in vivo* methylation (13, 19). The identification and mutagenesis of target arginines within these and other proteins will greatly enhance our understanding of mRNP complex formation as well as the coupling of transcription, processing, and export.

Acknowledgments—We thank Tina Beachy, Bill Steinhart, and the Biology 212 class at Bowdoin College for constructing the first RK mutants and Pam Silver, Elisa Shen, and Michael Yu for sharing strains. We thank Anita Corbett and Bruce Kohorn for critical reading of the manuscript and McBride laboratory members for helpful discussions throughout the project.

REFERENCES

1. Bedford, M. T., and Richard, S. (2005) *Mol. Cell* **18,** 263–272
2. Boisvert, F. M., Chenard, C. A., and Richard, S. (2005) *Sci. STKE* **2005,** re2
3. McBride, A. E., and Silver, P. A. (2001) *Cell* **106,** 5–8
4. Rajpurohit, R., Paik, W. K., and Kim, S. (1994) *Biochem. J.* **304,** 903–909
5. Valentini, S. R., Weiss, V. H., and Silver, P. A. (1999) *Rna* **5,** 272–280
6. Raman, B., Guarnaccia, C., Nadassy, K., Zakhariev, S., Pintar, A., Zanuttin, F., Frigyes, D., Acatrinei, C., Vindigni, A., Pongor, G., and Pongor, S. (2001) *Nucleic Acids Res.* **29,** 3377–3384
7. Denman, R. B. (2002) *Cell Mol. Biol. Lett.* **7,** 877–883

8. Lee, D. Y., Teyssier, C., Strahl, B. D., and Stallcup, M. R. (2005) *Endocr. Rev.* **26,** 147–170
9. Boffa, L. C., Karn, J., Vidali, G., and Allfrey, V. G. (1977) *Biochem. Biophys. Res. Commun.* **74,** 969–976
10. Dreyfuss, G., Kim, V. N., and Kataoka, N. (2002) *Nat. Rev. Mol. Cell. Biol.* **3,** 195–205
11. Nichols, R. C., Wang, X. W., Tang, J., Hamilton, B. J., High, F. A., Herschman, H. R., and Rigby, W. F. (2000) *Exp. Cell Res.* **256,** 522–532
12. Shen, E. C., Henry, M. F., Weiss, V. H., Valentini, S. R., Silver, P. A., and Lee, M. S. (1998) *Genes Dev.* **12,** 679–691
13. Green, D. M., Marfatia, K. A., Crafton, E. B., Zhang, X., Cheng, X., and Corbett, A. H. (2002) *J. Biol. Chem.* **277,** 7752–7760
14. Henry, M. F., and Silver, P. A. (1996) *Mol. Cell. Biol.* **16,** 3668–3678
15. Siebel, C. W., and Guthrie, C. (1996) *Proc. Natl. Acad. Sci. U. S. A.* **93,** 13641–13646
16. Wilson, S. M., Datar, K. V., Paddy, M. R., Swedlow, J. R., and Swanson, M. S. (1994) *J. Cell Biol.* **127,** 1173–1184
17. Flach, J., Bossie, M., Vogel, J., Corbett, A., Jinks, T., Willins, D. A., and Silver, P. A. (1994) *Mol. Cell. Biol.* **14,** 8399–8407
18. Lei, E. P., Krebber, H., and Silver, P. A. (2001) *Genes Dev.* **15,** 1771–1782
19. Yu, M. C., Bachand, F., McBride, A. E., Komili, S., Casolari, J. M., and Silver, P. A. (2004) *Genes Dev.* **18,** 2024–2035
20. Windgassen, M., Sturm, D., Cajigas, I. J., Gonzalez, C. I., Seedorf, M., Bastians, H., and Krebber, H. (2004) *Mol. Cell. Biol.* **24,** 10479–10491
21. Gary, J. D., and Clarke, S. (1998) *Prog. Nucleic Acids Res. Mol. Biol.* **61,** 65–131
22. Lee, M. S., Henry, M., and Silver, P. A. (1996) *Genes Dev.* **10,** 1233–1246
23. Senger, B., Simos, G., Bischoff, F. R., Podtelejnikov, A., Mann, M., and Hurt, E. (1998) *EMBO J.* **17,** 2196–2207
24. Chavez, S., Beilharz, T., Rondon, A. G., Erdjument-Bromage, H., Tempst, P., Svejstrup, J. Q., Lithgow, T., and Aguilera, A. (2000) *EMBO J.* **19,** 5824–5834
25. Strasser, K., Masuda, S., Mason, P., Pfannstiel, J., Oppizzi, M., Rodriguez-Navarro, S., Rondon, A. G., Aguilera, A., Struhl, K., Reed, R., and Hurt, E. (2002) *Nature* **417,** 304–308
26. Shen, E. C., Stage-Zimmermann, T., Chui, P., and Silver, P. A. (2000) *J. Biol. Chem.* **275,** 23718–23724
27. Xu, C., and Henry, M. F. (2004) *Mol. Cell. Biol.* **24,** 10742–10756
28. Hurt, E., Luo, M. J., Rother, S., Reed, R., and Strasser, K. (2004) *Proc. Natl. Acad. Sci. U. S. A.* **101,** 1858–1862
29. McBride, A. E., Weiss, V. H., Kim, H. K., Hogle, J. M., and Silver, P. A. (2000) *J. Biol. Chem.* **275,** 3128–3136
30. Rose, M. D., Winston, F., and Hieter, P. (1990) *Methods in Yeast Genetics: A Laboratory Course Manual*, Cold Spring Harbor Laboratory Press, Cold Spring Harbor, New York
31. Siniossoglou, S., Grandi, P., and Hurt, E. (1998) in *Cell Biology: A Laboratory Handbook* (Celis, J. E., ed) 2nd Ed., pp. 159–164 Academic Press, San Diego, CA
32. Sikorski, R. S., and Hieter, P. (1989) *Genetics* **122,** 19–27
33. Stemmler, E. A., Provencher, H. L., Guiney, M. E., Gardner, N. P., and Dickinson, P. S. (2005) *Anal. Chem.* **77,** 3594–3608
34. O'Connor, P. B., and Costello, C. E. (2000) *Anal. Chem.* **72,** 5881–5885
35. Clauser, K. R., Baker, P., and Burlingame, A. L. (1999) *Anal. Chem.* **71,** 2871–2882
36. Hellmuth, K., Lau, D. M., Bischoff, F. R., Kunzler, M., Hurt, E., and Simos, G. (1998) *Mol. Cell. Biol.* **18,** 6374–6386
37. Bossie, M. A., DeHoratius, C., Barcelo, G., and Silver, P. (1992) *Mol. Biol. Cell* **3,** 875–893
38. Marshall, A. G., Hendrickson, C. L., and Jackson, G. S. (1998) *Mass Spectrom. Rev.* **17,** 1–35
39. Rappsilber, J., Friesen, W. J., Paushkin, S., Dreyfuss, G., and Mann, M. (2003) *Anal. Chem.* **75,** 3107–3114
40. Gehrig, P. M., Hunziker, P. E., Zahariev, S., and Pongor, S. (2004) *J. Am. Soc. Mass Spectrom.* **15,** 142–149
41. Brame, C. J., Moran, M. F., and McBroom-Cerajewski, L. D. (2004) *Rapid Commun. Mass Spectrom.* **18,** 877–881
42. Qin, J., and Chait, B. T. (1995) *J. Am. Chem. Soc.* **117,** 5411–5412
43. Tsaprailis, G., Somogyi, A., Nikolaev, E. N., and Wysocki, V. H. (2000) *Int. J. Mass Spectrom.* **196,** 467–479
44. Lee, J. H., Cook, J. R., Pollack, B. P., Kinzy, T. G., Norris, D., and Pestka, S. (2000) *Biochem. Biophys. Res. Commun.* **274,** 105–111
45. Niewmierzycka, A., and Clarke, S. (1999) *J. Biol. Chem.* **274,** 814–824
46. Olsen, J. V., Ong, S. E., and Mann, M. (2004) *Mol. Cell Proteomics* **3,** 608–614
47. Smith, J. J., Rucknagel, K. P., Schierhorn, A., Tang, J., Nemeth, A., Linder, M., Herschman, H. R., and Wahle, E. (1999) *J. Biol. Chem.* **274,** 13229–13234
48. Yun, C. Y., and Fu, X. D. (2000) *J. Cell Biol.* **150,** 707–718
49. Gilbert, W., Siebel, C. W., and Guthrie, C. (2001) *Rna* **7,** 302–313
50. Najbauer, J., Johnson, B. A., Young, A. L., and Aswad, D. W. (1993) *J. Biol. Chem.* **268,** 10501–10509
51. Kwak, Y. T., Guo, J., Prajapati, S., Park, K. J., Surabhi, R. M., Miller, B., Gehrig, P., and Gaynor, R. B. (2003) *Mol. Cell* **11,** 1055–1066
52. Pellar, G. J., and DiMario, P. J. (2003) *Chromosoma* **111,** 461–469
53. Boisvert, F. M., Dery, U., Masson, J. Y., and Richard, S. (2005) *Genes Dev.* **19,** 671–676
54. Lee, Y. H., Coonrod, S. A., Kraus, W. L., Jelinek, M. A., and Stallcup, M. R. (2005) *Proc. Natl. Acad. Sci. U. S. A.* **102,** 3611–3616
55. Calnan, B. J., Tidor, B., Biancalana, S., Hudson, D., and Frankel, A. D. (1991) *Science* **252,** 1167–1171
56. Marfatia, K. A., Crafton, E. B., Green, D. M., and Corbett, A. H. (2003) *J. Biol. Chem.* **278,** 6731–6740
57. Kim, M., Ahn, S. H., Krogan, N. J., Greenblatt, J. F., and Buratowski, S. (2004) *EMBO J.* **23,** 354–364
58. Bucheli, M. E., and Buratowski, S. (2005) *EMBO J.* **24,** 2150–2160
59. Wang, Y., Wysocka, J., Sayegh, J., Lee, Y. H., Perlin, J. R., Leonelli, L., Sonbuchner, L. S., McDonald, C. H., Cook, R. G., Dou, Y., Roeder, R. G., Clarke, S., Stallcup, M. R., Allis, C. D., and Coonrod, S. A. (2004) *Science* **306,** 279–283
60. Cuthbert, G. L., Daujat, S., Snowden, A. W., Erdjument-Bromage, H., Hagiwara, T., Yamada, M., Schneider, R., Gregory, P. D., Tempst, P., Bannister, A. J., and Kouzarides, T. (2004) *Cell* **118,** 545–553
61. Pritzker, L. B., Joshi, S., Harauz, G., and Moscarello, M. A. (2000) *Biochemistry* **39,** 5382–5388
62. Doye, V., Wepf, R., and Hurt, E. C. (1994) *EMBO J.* **13,** 6062–6075
63. Henry, M., Borland, C. Z., Bossie, M., and Silver, P. A. (1996) *Genetics* **142,** 103–115